Thyroid nodules with indeterminate cytology: prospective comparison between ^{18}F-FDG-PET/CT, multiparametric neck ultrasonography, ^{99m}Tc-MIBI scintigraphy and histology

A Piccardo[1], M Puntoni[2], G Treglia[3], L Foppiani[4], F Bertagna[5], F Paparo[6], M Massollo[1], B Dib[1], G Paone[3], A Arlandini[7], U Catrambone[7], S Casazza[8], A Pastorino[8], M Cabria[1,*] and L Giovanella[3,*]

[1]Nuclear Medicine Unit and [2]Clinical Trial Unit, Office of the Scientific Director, Galliera Hospital, Genoa, Italy, [3]Department of Nuclear Medicine and PET/CT Centre, Oncology Institute of Southern Switzerland, Bellinzona, Switzerland, [4]Internal Medicine, Galliera Hospital, Genoa, Italy, [5]Department of Nuclear Medicine, University of Brescia and Spedali Civili di Brescia, Brescia, Italy, [6]Department of Radiology, [7]Department of Surgery, Thyroid Centre and [8]Department of Pathology, Galliera Hospital, Genoa, Italy
[*](M Cabria and L Giovanella contributed equally to this work)

Correspondence should be addressed to A Piccardo
Email
arnoldo.piccardo@galliera.it

European Journal of Endocrinology

Abstract

Purpose: To evaluate the role of ^{18}F-flurodeoxiglucose positron emission tomography/computed tomography (^{18}F-FDG-PET/CT) in predicting malignancy of thyroid nodules with indeterminate cytology.
Patients and methods: We analysed 87 patients who have been scheduled to undergo surgery for thyroid nodule with indeterminate cytology. All patients underwent ^{18}F-FDG-PET/CT, multiparametric neck ultrasonography (MPUS), and ^{99m}Tc-methoxyisobutylisonitrile scintigraphy (^{99m}Tc-MIBI-scan). Histopathology was the standard of reference.
We compared the sensitivity (SE), specificity (SP), accuracy (AC), positive (PPV) and negative predictive (NPV) values of ^{18}F-FDG-PET/CT with those of ^{99m}Tc-MIBI-scan and MPUS in detecting cancer. Univariate and multivariate analyses evaluated the association between each diagnostic tool and histopathology.
Results: On histopathology, 69 out of 87 nodules were found to be benign and 18 to be malignant. The SE, SP, AC, PPV and NPV of ^{18}F-FDG-PET/CT were 94, 58, 66, 37 and 98% respectively. The SE, AC and NPV of ^{18}F-FDG-PET/CT were significantly higher than those of MPUS and ^{99m}Tc-MIBI-scan. The association of both positive ^{18}F-FDG-PET/CT and MPUS (FDG+/MPUS+) showed significantly lower SE (61% vs 94%) and NPV (88% vs 98%) than ^{18}F-FDG-PET/CT alone, but significantly higher SP (77% vs 58%). On univariate analysis, ^{18}F-FDG-PET/CT and the combination of FDG+/MPUS+ and of FDG+/MIBI– were all significantly associated with histopathology. On multivariate analysis, only FDG+/MIBI– was significantly associated with histopathology.
Conclusion: The AC of ^{18}F-FDG-PET /CT in detecting thyroid malignancy is higher than that of ^{99m}Tc-MIBI-scan and MPUS. A negative ^{18}F-FDG-PET/CT correctly predicts benign findings on histopathology. The association of FDG+/MPS+ is significantly more specific than ^{18}F-FDG-PET/CT alone in identifying differentiated thyroid cancer. A positive ^{18}F-FDG-PET/CT is significantly associated with malignancy when qualitative ^{99m}Tc-MIBI-scan is rated as negative.

European Journal of Endocrinology
(2016) **174**, 693–703

www.eje-online.org
DOI: 10.1530/EJE-15-1199

Published by Bioscientifica Ltd.

Introduction

The finding of an undetermined cytology result after thyroid nodule fine-needle aspiration biopsy still remains a challenging situation, the management of which is still under debate. On the one hand, in these nodules the risk of malignancy reaches 15–30% (1), and a conservative approach may not be completely safe. On the other, more aggressive clinical management may involve over-treatment (i.e. total thyroidectomy or lobectomy) in more than 70% of patients.

Although various immunohistochemical markers (e.g. thyroperoxidase, galectin-3 and E-cadherin) have been proposed for the pre-surgical identification of malignancy, none has high enough accuracy to be used in routine clinical practice (2, 3). Similarly, several molecular markers, such as *RAS, BRAF, RET/PTC* and Pax8/PPARγ, have been explored, but, despite their high specificity in detecting malignancies, their sensitivity is too low (4, 5).

In this field, imaging tools characterized by high sensitivity and high negative predictive value (NPV) may be able to substantially reduce the number of patients undergoing inappropriate thyroidectomy. Multiparametric ultrasonography (MPUS), ^{99m}Tc methoxyisobutylisonitrile scintigraphy (^{99m}Tc MIBI scan) and ^{18}F-flurodeoxiglucose positron emission tomography/computed tomography (^{18}F-FDG PET/CT) are the principal diagnostic tools to have been proposed in recent years.

Several studies have investigated the role of US features in diagnosing indeterminate thyroid nodules. Although several US features have been shown to identify thyroid nodules at higher risk of malignancy (e.g. marked hypoechogenicity, irregular margins and microcalcifications), no definitive evidence has been obtained, and US alone is not recommended in the clinical management of indeterminate thyroid lesions (1, 6, 7, 8). In addition, although real-time elastography (RTE) has recently been reported to increase the sensitivity of US, it has suboptimal accuracy in diagnosing thyroid nodules previously classified as indeterminate (9). ^{99m}Tc-MIBI scan may be useful in the pre-surgical evaluation of thyroid nodules with undetermined cytology, and it has proved to be a specific tracer in identifying malignancy in non-oncocytic follicular lesions. However, it has not proved specific enough to distinguish benign oncocytic follicular lesions from malignant ones (10).

^{18}F-FDG PET/CT seems to be helpful in defining the nature of indeterminate nodules and has been reported to have a very high NPV (11, 12, 13, 14, 15, 16, 17). However, a recent study (18) on a considerable number of patients did not confirm the high NPV of ^{18}F-FDG PET/CT, and the authors concluded that this imaging tool did not add any diagnostic benefit to conventional US.

The aim of this two-centre study was to better clarify the role of ^{18}F-FDG PET/CT in detecting differentiated thyroid cancer (DTC) in patients with thyroid nodules with indeterminate cytology and to compare the results obtained with those of MPUS and ^{99m}Tc MIBI scan. We also assessed whether the combination of two of the three diagnostic tools could improve the accuracy of each single imaging test. A multivariate logistic analysis was also conducted to evaluate the association between malignancy and the results of each diagnostic tool, on adjusting for other clinical parameters such as age, nodule dimensions and thyroglobulin (Tg) levels. In addition, we tested the PPV of *BRAF* V600E mutation in patients with histologically proven DTC and the association between this mutation and ^{18}F-FDG and ^{99m}Tc MIBI uptake.

Patients and methods

Patient population

In our two centres (Galliera Hospital, Genoa, Italy and Oncology Institute of Southern Switzerland, Bellinzona, Switzerland), between November 2012 and March 2015 we

Table 1 Patients' characteristics.

	Mean (±S.D.)	Median (IQR)	Oncocytic lesions ($n=15$)	Nononcocytic lesions ($n=72$)
Age (years)	57±13	56 (49–67)		
TSH levels (IU/L)	1.7±0.9	1.6 (1.0–3.4)		
Tg levels (ng/mL)	202±445	71 (27.5–182)		
Dimensions of the nodule (mm)	24±13.4	20 (13–30)		
Dimensions of the thyroid carcinomas (mm)	26±16	23 (13–30)		
DTC, *n* (%)			3 (20)	15 (21)
Follicular adenomas, *n* (%)			8 (53)	13 (18)
Follicular hyperplasia, *n* (%)			4 (27)	44 (61)

Table 2 Sensitivity, specificity, positive predictive value (PPV), negative predictive value (NPV) and accuracy in detecting thyroid malignancy using multiparametric ultrasonography (MPUS) alone ^{18}F-FDG-PET/CT alone and ^{99m}Tc-methoxyisobutylisonitrile scintigraphy-scan alone.

	PET/CT (%)	MPUS (%)	^{99m}Tc-MIBI-scan (%)
Sensitivity	94	50 (0.02)	56 (0.01)
Specificity	58	52 (0.6)	52 (0.4)
PPV	37	21 (0.1)	23 (0.17)
NPV	98	80 (0.01)	82 (0.03)
Accuracy	66	52 (0.01)	53 (0.02)

Values in parentheses indicate *P* value vs PET/CT.

prospectively enrolled 87 patients (23 males, 64 females) who had been scheduled to undergo thyroidectomy for thyroid nodules with undetermined cytology according the Società Italiana di Anatomia e Citologia Patologica-International Academy of Pathology classification (2010) (1). The inclusion criteria were as follows: thyroid nodule with a diameter of >1 cm, TSH levels between 1 and 4 mUI/l and undetectable thyroperoxidase and Tg auto-antibodies. The study included 74 patients at Galliera Hospital and 13 patients at Oncology Institute of Southern Switzerland.

Our institutional review board approved the study and all patients gave their written informed consent.

Imaging modalities

All patients underwent MPUS, ^{99m}Tc MIBI scan and ^{18}F-FDG PET/CT within 1 day of each other. Image acquisition was performed according to standard procedures.

First all patients were examined by using neck US (LOGIQ S8 General Electric Medical Systems, Milwaukee, WI, USA). The US parameters evaluated included, nodule diameters, structure (i.e. solid or mixed) echogenicity (hypoechoic, hyperechoic, isoechoic), presence or absence of irregular margins and presence or absence of microcalcifications. Following Power Doppler US analysis, nodule blood flow was classified as negative in case of absent or presence of marked peripheral blood flow and positive in case of intralesional blood flow. The elastic properties of thyroid nodules were assessed by means of RTE. This technique measures mechanically probe-induced deformation (strain) of structures and tissues examined in the B-mode ultrasound image, producing colour-coded maps of the strain distribution (i.e. elastograms) that reflect tissue elasticity (19, 20).

The RTE module implemented in our ultrasound system generates a colour map in which hard tissue areas appear blue, intermediate tissue areas are green, and soft tissue areas are red. Elastograms were obtained by placing the probe on the long axis of each thyroid nodule and RTE images were produced applying gentle pulse compression on the skin (19).

RTE images were assessed by means of a dychotomous qualitative analysis, dividing thyroid nodules into soft and hard groups. A nodule softer than, or with the same stiffness of the surrounding parenchyma, was considered soft (with a green, yellow or green appearance on the colour-coded map). By converse, a nodule harder/stiffer than the adjacent thyroid parenchyma (with a blue appearance on the colour-coded map) was considered hard.

^{99m}Tc MIBI scans were obtained 20 and 120 min after the injection of 400 MBq of ^{99m}Tc MIBI (Cardiolite, Bristol-Myers-Squibb, North Billerica, MA, USA). All scan images were obtained in the anterior projection of the neck using a gamma camera (Millenium, GE Medical Systems, Milwaukee, WI, USA or ECAM, Siemens Medical Solutions, Knoxville, TN, USA) equipped with a high-resolution, parallel-hole, low-energy high-resolution collimator. The images were obtained in a 256×256 matrix using a digital zoom of 1.8. The acquisition time was set to 900 s with a 20% window centred at 140 keV in all cases.

Table 3 Sensitivity, specificity, positive predictive value (PPV), negative predictive value (NPV) and accuracy in detecting thyroid malignancy using ^{18}F-flurodeoxiglucose positron emission tomography/computed tomography alone and each feature of multiparametric ultrasonography.

		Multiparametric US					
	PET/CT (%)	Solid lesion (%)	Hypoechogenicity (%)	Irregular margins (%)	Microcalcification (%)	Hypervascularization (%)	Stiffness (%)
Sensitivity	94	94 (1)	67 (0.12)	33 (0.001)	28 (0.001)	22 (0.00001)	47 (0.03)
Specificity	58	13 (0.0001)	43 (0.13)	77 (0.04)	75 (0.04)	65 (0.48)	49 (0.07)
PPV	37	22 (0.09)	24 (0.18)	27 (0.58)	23 (0.28)	14 (0.06)	20 (0.14)
NPV	98	90 (0.35)	83 (0.04)	82 (0.01)	80 (0.008)	76 (0.003)	77 (0.007)
Accuracy	66	30 (0.0001)	48 (0.003)	68 (0.7)	66 (1)	56 (0.3)	49 (0.006)

Values in parentheses indicate *P* value vs PET/CT.

Table 4 Sensitivity, specificity, positive predictive value (PPV), negative predictive value (NPV) and accuracy in detecting thyroid malignancy using ^{18}F-flurodeoxiglucose positron emission tomography/computed tomography alone and the diagnostic associations between MPUS, ^{99m}Tc-MIBI scan and ^{18}F-FDG-PET/CT.

		Diagnostic association		
	PET/CT (%)	FDG+/MIBI+ (%)	FDG+/MIBI− (%)	FDG+/MPUS+ (%)
Sensitivity	94	56 (0.01)	39 (0.002)	61 (0.03)
Specificity	58	64 (0.12)	94 (0.0001)	77 (0.002)
PPV	37	29 (0.48)	64 (0.17)	41 (0.8)
NPV	98	85 (0.03)	86 (0.05)	88 (0.14)
Accuracy	66	62 (0.54)	83 (0.01)	74 (0.17)

Values in parentheses indicate *P* value vs PET/CT.

^{18}F-FDG PET/CT of the neck was performed 50 min after the injection of tracer; data were acquired in the three-dimensional mode by means of two dedicated 16-slice PET/CT system (in one Nuclear Medicine Department with Discovery ST, GE Medical Systems; in the second with Biograph 16 Siemens Medical Solutions). The activity administered was 111 MBq. ^{18}F-FDG PET of the neck was performed in one bed positions (5-min emissions per bed position) and images were reconstructed by using an iterative algorithm. A non-diagnostic CT scan (low-dose CT with 120 kV, 80 mA, 0.6 s per rotation) was used for attenuation correction and anatomical localization of the hot spots of the ^{18}F-FDG PET study. Motion correction software was not available.

Image interpretation

MPUS US was considered positive in the presence of at least three of these characteristics; solid nodule, hypoechoic nodule, irregular margins, microcalcifications, intralesional blood flow and increased nodule stiffness.

^{18}F-FDG-PET/CT was interpreted visually and semiquantitatively using the maximum standardized uptake value (SUV-max). However, no SUV-max cut-off value has been introduced and SUV was calculated for each lesion just to support visual interpretation. On ^{18}F-FDG-PET/CT, any focal uptake above thyroid parenchyma, corresponding to the nodule with cytological undetermined results, was considered as positive. In addition nodule/normal thyroid gland SUV-max (SUV ratio) was quantitatively assessed by using regions of interest (ROIs) drawn on the images. On ^{99m}Tc-MIBI image any early and late focal uptake above thyroid parenchyma (i.e. nodule/thyroid parenchyma ratio >1), corresponding to the nodule with cytological undetermined results, was considered as positive (21, 22).

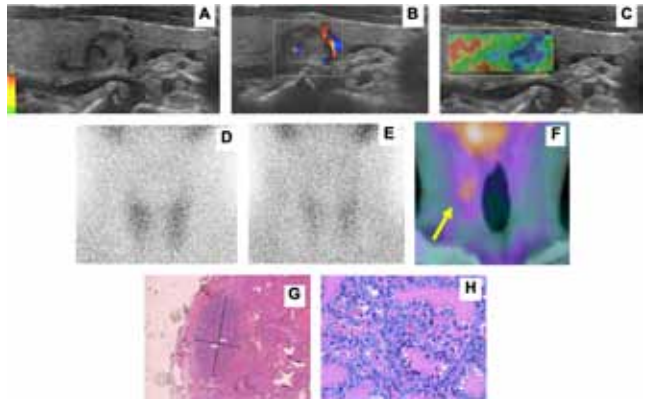

Figure 1
(A) 13 mm isoechoic solid nodule characterized by well-defined margins and without microcalcifications, located in the inferior part of the right thyroid lobe in the subcapsular region (A). The vascularization of the nodule was peripheral on colour-Doppler evaluation (B) and the only suspected feature was the increased stiffness found on real-time elastography (C). ^{99m}Tc-methoxyisobutylisonitrile scintigraphy scan did not show focal uptake in the right thyroid lobe either 20 min (D) or 1 h after tracer injection (E). By contrast, ^{18}F-flurodeoxiglucose positron emission tomography/computed tomography showed focal uptake (F) corresponding to the small thyroid nodule detected by US. Histopathology (haematoxylin-eosin stain, 4× (G) and (H) haematoxylin-eosin stain, 10×) revealed a small subcaspular papillary carcinoma.

Diagnostic patterns

In order to evaluate the additional value of diagnostic associations between MPUS, ^{99m}Tc-MIBI scan and ^{18}F-FDG-PET/CT, we defined three different patterns as follows:

(i) positive ^{18}F-FDG-PET/CT and positive MPUS (FDG+/MPUS+),
(ii) positive ^{18}F-FDG-PET/CT and positive ^{99m}Tc-MIBI scan (FDG+/MIBI+), and
(iii) positive ^{18}F-FDG-PET/CT and negative ^{99m}Tc-MIBI scan (FDG+/MIBI−).

Standard of reference and *BRAF* mutation analysis

For all patients histopathological results were available. In all 18 DTC patients, DNA was extracted from samples after

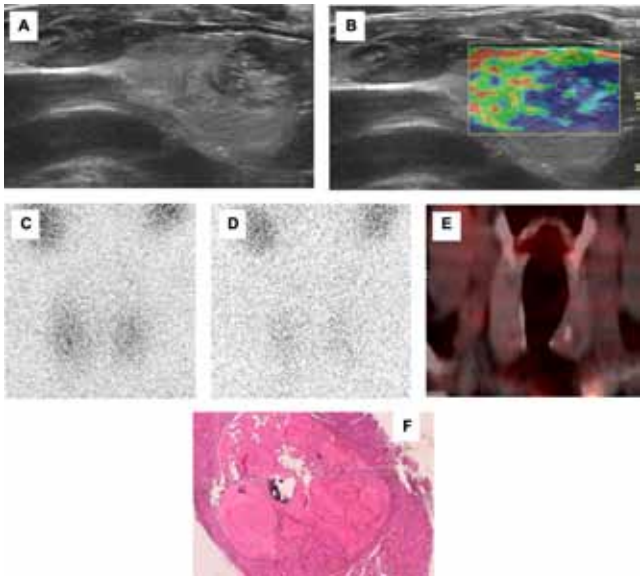

Figure 2

(A) 25 mm hypoechoic solid nodule of the left lobe, characterized by undefined margins and multiple microcalcifications (A). The vascularization of the nodule was not significantly increased on colour-Doppler evaluation (not shown) and increased stiffness was found on real-time elastography (B). ^{99m}Tc-methoxyisobutylisonitrile scintigraphy scan did not show uptake in the left thyroid lobe either 20 min (C) or 1 h (D) after tracer injection. ^{18}F-flurodeoxiglucose positron emission tomography/computed tomography (E) did not show any uptake corresponding to the thyroid nodule detected by US. Histopathology revealed a hyperplastic nodule characterized by micro- and macrocalcifications (haematoxylin-eosin stain, 4×) (F).

micro-dissection by using the QIAamp DNA FFPE Tissue Kit (Qiagen, Hilden, Germany) according to the manufacturer's instructions and amplified through Rotor-Gene 6000 real time PCR machine (Corbett Research, Eaton Socon, St. Neots, U.K.). *BRAF* mutation analysis was performed by means of Pyrosequencing platform 'PyroMark Q96 ID System' (Qiagen) using the commercial 'Anti-EGFR MoAb Response (*BRAF* status)' Kit (Diatech Pharmacogenetics, Jesi, Italy). This system allows to identify all variants of codon 600 of exon 15, including the most frequent one V600E (Val600Glu). Thus, all DTC patients were classified as *BRAF* V600E mutated or *BRAF* wild-type.

Statistical analysis

Descriptive statistics used for continuous factors where mean and standard deviation, median and interquartile range; in case of categorical factors, absolute and relative frequencies (%) were adopted. Sensitivity (SE), specificity (SP), positive predictive value (PPV), NPV and accuracy (AC, defined as the number of ((true positives)+(true negatives))/total) were calculated and compared between the each diagnostic techniques and the gold standard, as previously defined (histopathology). Fisher's exact test was used to compare independent diagnostics indicators (PPV, NPV); McNemar test was used for comparison of paired diagnostics indicators (SE, SP, AC).

Logistic regression modelling was adopted to calculate odds ratios (ORs) and Wald test to estimate and test the association between the histopathology assessment (positive/negative) and each of the diagnostic techniques/parameters considered. ORs from univariate models were adjusted only for age and dimensions of nodule; ORs from multivariate models were adjusted for age, dimensions of nodule and for all other factors with a Wald *P*-value <0.3 in the univariate analysis. In case of high correlated factors, to avoid multicollinearity, we included in the multivariate model only the most significant factors from the univariate analysis.

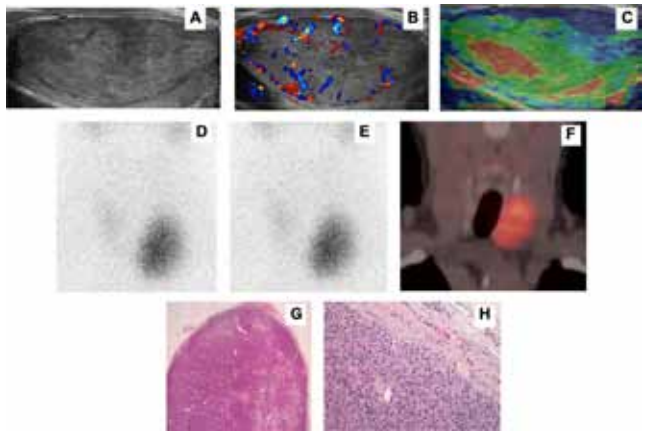

Figure 3

(A) 39 mm isoechoic solid nodule of the left thyroid lobe, characterized by well-defined margins and without microcalcifications (A). The vascularization of the nodule was significantly increased on colour-Doppler evaluation (B) and a high level of elasticity was found on real-time elastography (C). ^{99m}Tc-methoxyisobutylisonitrile scintigraphy scan showed intense uptake in the left thyroid lobe 20 min (D) and 1 h after tracer injection (E). ^{18}F-flurodeoxiglucose positron emission tomography/computed tomography showed focal uptake corresponding to the thyroid nodule detected by US (F). Histopathology revealed a follicular adenoma (haematoxylin-eosin stain, 4× (G) and haematoxylin-eosin stain, 10× (H).

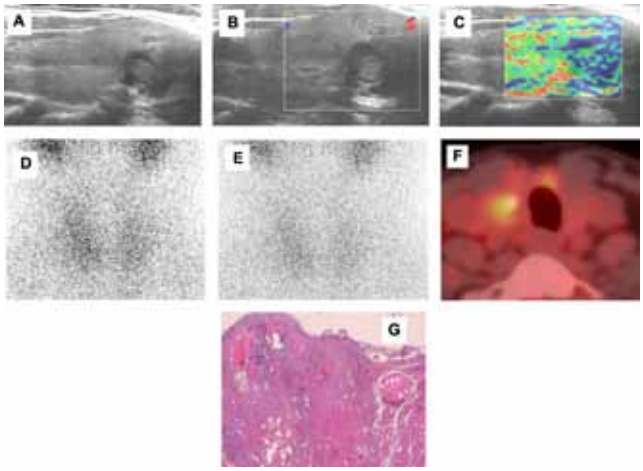

Figure 4

(A) 12 mm hypoechoic solid nodule characterized by irregular margins located in the inferior part of the right thyroid lobe in the subcapsular region (A). The vascularization of the nodule was absent on colour-Doppler evaluation (B) and stiffness was mildly increased on real-time elastography (C). ^{99m}Tc-methoxyisobutylisonitrile scintigraphy scan did not show focal uptake in the right thyroid lobe either 20 min (D) or 1 h (E) after tracer injection. By contrast, ^{18}F-flurodeoxiglucose positron emission tomography/computed tomography (F) showed focal uptake corresponding to the thyroid nodule detected by US. Histopathology (haematoxylin-eosin stain, 4×) revealed a papillary carcinoma (G).

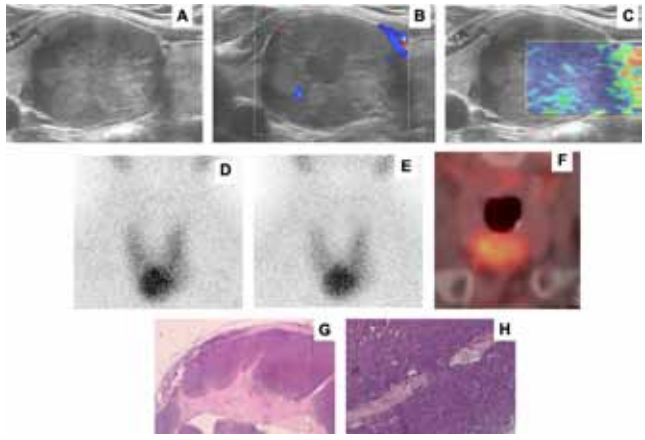

Figure 5

(A) 35 mm hypoechoic solid nodule of the isthmus, characterized by defined margins and without microcalcifications (A). The vascularization of the nodule was not significantly increased on colour-Doppler evaluation (B) and increased stiffness was found on real-time elastography (C). ^{99m}Tc-methoxyisobutylisonitrile scintigraphy scan showed intense uptake in the left thyroid lobe 20 min (D) and 1 h after tracer injection (E). ^{18}F-flurodeoxiglucose positron emission tomography/computed tomography (F) showed focal uptake corresponding to the thyroid nodule detected by US. Histopathology (haematoxylin-eosin stain, 4× (G) and 10× (H)) revealed a follicular carcinoma.

All analyses were conducted using Stata (version 13, StataCorp, College Station, TX, USA) software. Two-tailed probabilities were reported and the *P* value of 0.05 was used to define nominal statistical significance.

Results

At histopathology 69 out of 87 nodules (79%) were found to be benign (48 follicular hyperplasia and 21 follicular adenomas) and 18 (21%) were malignant, including 13 papillary carcinomas and five follicular carcinomas (FTC). Six patients with pT1, six patients with pT2, and six patients with pT3 were found. Patients' characteristics are summarized in Table 1. Out of 41, only one patient with negative ^{18}F-FDG-PET/CT had final histological diagnosis of malignancy. In 69 out of 87 patients concordant findings were detected by ^{18}F-FDG-PET/CT and ^{99m}Tc-MIBI-scan. The SE, SP, AC, positive (PPV), and negative predictive (NPV) values of ^{18}F-FDG-PET/CT in detecting cancer were 94, 58, 66, 37 and 98%, respectively. The SE, AC and NPV of ^{18}F-FDG-PET/CT were significantly higher than those of MPUS and ^{99m}Tc-MIBI-scan (Table 2 and Figs 1 and 2). When each US parameter was separately considered, the sensitivity of ^{18}F-FDG-PET was significantly higher than that related to the presence of microcalcifications, irregular margins, intralesional blood flow and increased nodule stiffness (Table 3). On the contrary, the specificity of microcalcifications and irregular margins was higher than that of ^{18}F-FDG-PET/CT (Tables 3 and 4).

The FDG+/MIBI+ pattern (Fig. 3) presented similar accuracy (62% vs 66%) but a significantly lower sensitivity (56% vs 94%) and NPV (85% vs 98%) than that of ^{18}F-FDG-PET/CT alone (Table 4). On the other hand, the FDG+/MIBI– (Fig. 4) presented a significantly higher specificity (94% vs 58%) and accuracy (83% vs 66%) than that of ^{18}F-FDG-PET/CT alone but a significantly lower sensitivity (39% vs 94%) (Table 4).

The FDG+/MPUS+ pattern (Fig. 5) showed a significantly lower sensitivity (61% vs 94%) and NPV (88% vs 98%) but a significantly higher specificity (77% vs 58%) than that of ^{18}F-FDG-PET/CT alone (Table 4).

BRAF V600E mutation status was analysed in all 18 histologically proven DTC patients and we found only

Table 5 Logistic regression analysis: dependent variable: positive(='1')/negative ('0') histology.

Factor	*n* (%)	OR_u (*P* value)	OR_m (*P* value)
US structure			
Cystic	10 (11)	1.0	1.0
Solid	77 (89)	3.5 (0.3)	33.4 (0.3)
Ecogenity			
Iso-hyperechogenity	36 (41)	1.0	–
Hypoechogenity	51 (59)	1.6 (0.4)	
Microcalcifications			
Absence	65 (75)	1.0	–
Presence	22 (25)	1.1 (0.8)	
Margins			
Regular	65 (75)	1.0	–
Irregular	22 (25)	1.6 (0.4)	
Hypervascularization			
Absence	59 (68)	1.0	1.0
Presence	28 (32)	0.5 (0.2)	0.8 (0.9)
Elastography			
Softness	35 (50)	1.0	–
Stiffness	35 (50)	0.8 (0.8)	
Multiparametric US			
Negative	45 (52)	1.0	–
Positive	42 (48)	1.2 (0.8)	
MIBI			
No uptake	44 (51)	1.0	–
Uptake	43 (49)	1.2 (0.8)	
PET			
No uptake	41 (47)	1.0	1.0
Uptake	46 (53)	28.4 (0.002)	6.2 (0.16)
FDG+/MPUS+			
Negative	60 (69)	1.0	1.0
Positive	27 (31)	6.5 (0.002)	2.3 (0.3)
FDG+/MIBI+			
Negative	52 (60)	1.0	–
Positive	35 (40)	2.2 (0.2)	
FDG+/MIBI–			
Negative	76 (87)	1.0	1.0
Positive	11 (13)	21.3 (<0.001)	7.5 (0.05)
SUV ratio	*n*=86	1.006 (0.9)	–
MIBI ratio	*n*=78	1.4 (0.7)	–
Tg*	*n*=72	1.0007 (0.2)	1.0008 (0.09)

OR_u, odds ratios from a univariate logistic regression model adjusted for age and dimensions of nodule; OR_m, odds ratios from a multivariate logistic regression model adjusted for age, dimensions of nodule and all other factors which had a *P* value<0.3 in the univariate analysis. In case of high correlated factors, to avoid multicollinearity, we included in multivariate model only the most significant factors in the univariate analysis.
*Tg, SUV ratio and MIBI ratio were continuous factors: consequently the OR stands for 1-unit increase.

four *BRAF*-mutated and 14 wild-type (PPV 22%) patients. We did not find any significant difference (*P*=0.9) in terms of SUV ratio between *BRAF*-mutated and the wild-type patients. On the other hand, when MIBI uptake was taken into account, we found that *BRAF*-mutated patients presented a significantly lower MIBI ratio (*P*=0.047) than wild-type patients. Only FDG-negative DTC patient did not show *BRAF* mutation.

On univariate analysis, ^{18}F-FDG-PET/CT positive results, FDG+/MIBI– and FDG+/MPUS+ patterns were all significantly associated with malignancy at histopathology (Table 5 and Fig. 3). Neither SUV ratio nor MIBI ratio was significantly associated with malignancies. In a multivariate logistic regression model adjusted for age, dimensions of nodule and all other factors which had a *P* value <0.3 in the univariate analysis, we found that only the FDG+/MIBI– pattern (*P*=0.05) was associated with DTC. Moreover, a trend towards the level of statistical significance was found between Tag levels and DTC (*P*=0.09; Table 5).

Discussion

We prospectively compared the ability of ^{18}F-FDG PET/CT, MPUS and ^{99m}Tc-MIBI-scan to characterize thyroid nodules with indeterminate cytology in 87 patients. To the best of our knowledge, this is the first time that such a comparison has been made.

First our study showed that the overall SE and AC of ^{18}F-FDG PET/CT are significantly higher than those of both MPUS and ^{99m}Tc-MIBI-scan. The most important datum that we want to underline is the very high NPV of ^{18}F-FDG PET/CT (98%), which is significantly higher than those of MPUS, each single US and ^{99m}Tc-MIBI-scan. By contrast, as expected, we found a low PPV of ^{18}F-FDG PET/CT (38%) confirming previous data (23, 24). All in all, a negative ^{18}F-FDG PET/CT significantly reduces inappropriate thyroidectomies while positive nodules deserve lobectomy and histological examination. The full implementation of this diagnostic and clinical approach in patients with indeterminate thyroid nodules may reduce costs and increase the patients' quality of life (25).

In our patients MPUS had suboptimal levels of sensitivity (50%) and specificity (52%) while in a similar series Deandreis *et al.* (18) found higher sensitivity (82%) and lower specificity (47%). This finding is probably related to the higher prevalence of malignancies and less stringent definition of suspicious thyroid nodules on MPUS in the latter study. Considering each single US feature, we found, in agreement with Yoo *et al.* (26), that the most sensitive US parameters were solid nodule structure (94%) and hypoechogenicity (67%) with no difference in terms of sensitivity from ^{18}F-FDG PET/CT. Interestingly, irregular margins and microcalcifications were the most specific US parameters and showed a significantly higher specificity than that of ^{18}F-FDG PET/CT. Like Yoo *et al.* (26), we found that nodule internal hypervascularity was not sensitive and specific enough to correctly identify

thyroid malignancy. This finding is probably related to the intense internal hypervascularity of follicular adenomas (24% of all nodules in our patients) commonly detected on US (27). At the same time, we confirmed (9) that RTE has suboptimal accuracy in diagnosing thyroid nodules previously classified as indeterminate and is unable to select patients for surgery.

Secondly, we found that ^{99m}Tc-MIBI-scan had levels of AC (53%) and SE (56%) significantly lower than those of ^{18}F-FDG PET/CT. Although one meta-analysis has reported the diagnostic performance of ^{99m}Tc-MIBI-scan in predicting the malignancy of thyroid nodules (28), only two prospective studies (10, 29) have evaluated the diagnostic role of ^{99m}Tc-MIBI-scan in thyroid nodules with indeterminate cytology. The authors found higher SE and AC than those reported in our series. Some possible explanations of these discrepancies may be cited. In their paper, the authors included only patients with cold nodules on ^{99m}Tc-pertechnetate thyroid scan. Moreover, selecting patients with class IV Bethesda at cytology (i.e. follicular proliferations '*sensu strictu*') (30), their series were characterized by a higher prevalence of DTC (26–37%). Indeed, most neoplasms were follicular cancers. In this study, a different cytological classification was adopted, resulting in a lower prevalence of malignancy with more papillary cancers than follicular cancers detected. Finally, Saggiorato *et al*. (10) and Giovanella *et al*. (29) assessed the tracer washout by a semi-quantitative analysis to calculate the retention or washout index, respectively. Of importance, only semi-quantitative analysis of tracer kinetic proved to be able to rule-out surgery.

The only one other paper (31) comparing ^{99m}Tc-MIBI-scan and ^{18}F-FDG PET/CT in the preoperative evaluation of thyroid nodules reported, using interpretation criteria similar to that adopted by Saggiorato *et al*. and Giovanella et al., that these imaging techniques had the same SE and similar NPV. Indeed, Sager *et al*. (31) studied a limited number of patients (n=23) who presented larger thyroid nodules (median 32 mm vs 24 mm) and larger thyroid malignancies (median 30 mm vs 23 mm) than those of our series and cytology was not considered in patient selection.

Overall, accuracy of ^{99m}Tc-MIBI-scan may have been underestimated in our patients and no conclusions can be drawn on the superiority of ^{18}F-FDG PET/CT over ^{99m}Tc-MIBI-scan. However, the MIBI semiquantitative analysis is time-consuming and, at least partially, an operator-dependent technique, especially with regard to the definition of the ROIs. Furthermore, this technique is partially dependent on the instruments used and the peculiarities of the local patient population. Therefore, each laboratory needs to optimize the protocol and to define its normal reference values. ^{18}F-FDG PET/CT procedure is more standardized and qualitative analysis is relatively simple when compared with ^{99m}Tc-MIBI quantification and interpretation.

Anyway, molecular imaging (^{99m}Tc-MIBI-scan) proved superior to molecular testing in differentiating benign from malignant follicular neoplasm also in terms of cost-effectiveness (29, 32).

Thirdly, on considering the combined pattern of FDG+/MPUS+, we found that the specificity in detecting DTC was significantly higher than that of ^{18}F-FDG PET/CT alone. This finding, which has never been reported before, may improve the well-known low specificity of ^{18}F-FDG PET/CT, suggesting which patients are more suitable for thyroidectomy. A similarly important finding emerged when we considered FDG+/MIBI−. The specificity of this metabolic pattern, which reached 94%, was significantly higher than that of ^{18}F-FDG PET/CT alone. In particular, when we conducted a logistic analysis to evaluate the association between malignancy and the results of each diagnostic tool or diagnostic association, after adjusting for other clinical parameters such as age, nodule dimensions and Tg levels, we found that, at the univariate level, ^{18}F-FDG PET/CT, FDG+/MIBI− and FDG+/MPUS+ were all significantly associated with histopathology. However, on multivariate analysis, only the FDG+/MIBI− pattern was associated with malignancy. However, in order to better evaluate the real diagnostic impact of this pattern (FDG+/MIBI−) and to ascertain a real pathophysiological substrate, further studies on a larger sample population are needed.

On multivariate analysis, we found an interesting trend towards a significant association between Tg levels (expressed as a continuous variable) and malignancy. This is in agreement with what was reported by a recent meta-analysis (33), in which the preoperative Tg value was deemed to be an independent predictor of thyroid cancer and should be considered especially in the case of thyroid nodules with indeterminate cytology.

Fourthly, considering the connection between *BRAF* V600E mutation and mortality (34) and the inverse correlation between survival and FDG uptake in DTC patients (35, 36), we tested the association between primary thyroid tumour uptake (expressed in terms of SUV ratio) and *BRAF* V600E mutation *in vivo*; to our knowledge, this was the first such test. Although this association has recently been reported in patients with DTC metastases (37), we did

not find any correlation between *BRAF* V600E mutation and FDG uptake. However, we tested this association only on a relatively small number of patients with DTC, a high percentage of which were FTC, mostly at an early stage, and often characterized by an indolent behaviour (38); in such cases, a low number of *BRAF* V600E mutations should be expected *a priori*, as indeed we found (22%).

By contrast, patients with *BRAF* mutations presented a significantly lower MIBI ratio than wild-type patients. This association may have been influenced by the low numbers of *BRAF* mutations; nevertheless, in this case, we found a significant *P* value. One possible, albeit speculative, explanation could be related to the low MIBI ratio evaluated in the late images. This tracer behaviour may be associated with the multi-drug resistance protein often expressed by DTC and, in some cases, related to poor prognosis (39). In this setting, DTC with low MIBI uptake in late images might be more aggressive, thus presenting *BRAF* mutation. However, as previously stated, absolute wash-out assessment is mandatory to prove an efflux of the tracer from the tumour while our analysis was based on relative uptake of normal thyroid and tumour tissue, respectively. As a consequence further studies are required to test this hypothesis.

Finally, we found that *BRAF* mutation had low NPV in detecting DTC. Thus, we confirmed what was reported in a recent systematic review, i.e. a marginal value of this biomarker in detecting malignancy in nodules with indeterminate cytology reports (4).

Limitations

Despite our encouraging results, some limitations should be noted. Although the number of patients included in this study was high, the number of DTC patients, as expected, was relatively low. A higher number of DTC could have helped to better evaluate the real diagnostic impact of ^{18}F-FDG PET/CT in this challenging scenario. However, this is an intrinsic limitation of all studies investigating the role of imaging in thyroid nodules with indeterminate cytology.

The diagnostic sensitivity of ^{99m}Tc-MIBI-scan and, more generally its accuracy, may have been affected by our analysis. In addition, as we did not preselect patients on the basis of cold nodule on ^{99m}Tc-pertechnetate scintigraphy, we could not apply the visual analysis proposed by Hurtado-Lopez *et al.* (i.e. any nodular uptake of ^{99m}Tc-MIBI>^{99m}Tc-pertechnetate is considered positive), which significantly increases the SE and NPV of ^{99m}Tc-MIBI thyroid scan (40).

Conclusion

The accuracy of ^{18}F-FDG-PET/CT in detecting thyroid malignancy is higher than that of qualitative ^{99m}Tc-MIBI-scan and MPUS. A negative ^{18}F-FDG-PET/CT correctly predicts a benign finding on histopathology. The pattern FDG+ is significantly associated with malignancy when qualitative MIBI scan is rated as negative. The association of FDG+/MPUS+ is significantly more specific than ^{18}F-FDG-PET/CT alone in identifying DTC.

Declaration of interest
The authors declare that there is no conflict of interest that could be perceived as prejudicing the impartiality of the research reported.

Funding
This research did not receive any specific grant from any funding agency in the public, commercial or not-for-profit sector.

References

1 Fadda G, Basolo F, Bondi A, Bussolati G, Crescenzi A, Nappi O, Nardi F, Papotti M, Taddei G, Palombini L & SIAPEC-IAP Italian Consensus Working Group. Cytological classification of thyroid nodules. Proposal of the SIAPEC-IAP Italian Consensus Working Group. *Pathologica* 2010 **102** 405–408.

2 Orlandi F, Saggiorato E, Pivano G, Puligheddu B, Termine A, Cappia S, De Giuli P & Angeli A. Galectine-3 is a presurgical marker of human thyroid carcinoma. *Cancer Research* 1998 **58** 3015–3020.

3 Bartolazzi A, Gasbarri A, Papotti M, Bussolati G, Lucante T, Khan A, Inohara H, Marandino F, Orlandi F, Nardi F *et al.* Application of an immunodiagnostic method for improving preoperative diagnosis of nodular thyroid lesions. *Lancet* 2001 **357** 1644–1650.

4 Trimboli P, Treglia G, Condorelli E, Romanelli F, Crescenzi A, Bongiovanni M & Giovanella L. BRAF-mutated carcinomas among thyroid nodules with prior indeterminate FNA report: a systematic review and meta-analysis. *Clinical Endocrinology* 2016 **84** 315–320. (doi:10.1111/cen.12806).

5 Ohori NP, Nikiforova MN, Schoedel KE, LeBeau SO, Hodak SP, Seethala RR, Carty SE, Ogilvie JB, Yip L & Nikiforov YE. Contribution of molecular testing to thyroid fine-needle aspiration cytology of "follicular lesion of undetermined significance/atypia of undetermined significance". *Cancer Cytopathology* 2010 **25** 17–23. (doi:10.1002/cncy.20063)

6 Trimboli P, Condorelli E, Catania A & Sorrenti S. Clinical and ultrasound parameters in the approach to thyroid nodules cytologically classified as indeterminate neoplasm. *Diagnostic Cytopathology*. 2009 **37** 783–785. (doi:10.1002/dc.v37:10)

7 Gharib H, Papini E, Paschke R, Duick DS, Valcavi R, Hegedus L & Vitti P. AACE/AME/ETA Task Force on Thyroid Nodules, American Association of Clinical Endocrinologists, Associazione Medici Endocrinologi, and European Thyroid Association Medical guidelines for clinical practice for the diagnosis and management of thyroid nodules: executive summary of recommendations. *Endocrine Practice* 2010 **16** 468–475. (doi:10.4158/EP.16.3.468)

8 Cooper DS, Doherty GM, Haugen BR, Kloos RT, Lee SL, Mandel SJ, Mazzaferri EL, McIver B, Pacini F, Schlumberger M *et al*. Revised American Thyroid Association management guidelines for patients with thyroid nodules and differentiated thyroid cancer. *Thyroid* 2009 **19** 1167–1214. (doi:10.1089/thy.2009.0110)

9 Trimboli P, Treglia G, Sadeghi R, Romanelli F & Giovanella L. Reliability of real-time elastography to diagnose thyroid nodules previously read at FNAC as indeterminate: a meta-analysis. *Endocrine* 2015 **50** 335–343. (doi:10.1007/s12020-014-0510-9)

10 Saggiorato E, Angusti T, Rosas R, Martinese M, Finessi M, Arecco F, Trevisiol E, Bergero N, Puligheddu B, Volante M *et al*. 99mTc-MIBI Imaging in the presurgical characterization of thyroid follicular neoplasms: relationshipto multidrug resistance protein expression. *Journal of Nuclear Medicine* 2009 **50** 1785–93. (doi:10.2967/jnumed.109.064980)

11 Kresnik E, Gallowitsch HJ, Mikosch P, Stettner H, Igerc I, Gomezi, Kumnig G & Lind P. Fluorine-18-fluorodeoxyglucose positron emission tomography in the preoperative assessment of thyroid nodules in an endemic goiter area. *Surgery* 2003 **133** 294–299. (doi:10.1067/msy.2003.71)

12 de Geus-Oei LF, Pieters GF, Bonenkamp JJ, Mudde AH, Bleeker- Rovers CP, Corstens FH & Oyen WJ. 18F FDG PET reduces unnecessary hemithyroidectomies for thyroid nodules with inconclusive cytologic results. *Journal of Nuclear Medicine* 2006 **47** 770–775.

13 Sebastianes FM, Cerci JJ, Zanoni PH, Soares J Jr, Chibana LK, Tomimori EK, de Camargo RY, Izaki M, Giorgi MC, Eluf-Neto J *et al*. Role of 18F fluorodeoxyglucose positron emission tomography in preoperative assessment of cytologically indeterminate thyroid nodules. *Journal of Clinical Endocrinology and Metabolism* 2007 **92** 4485–4488. (doi:10.1210/jc.2007-1043)

14 Hales NW, Krempl GA & Medina JE. Is there a role for fluorodeoxyglucose positron emission tomography/computed tomography in cytologically indeterminate thyroid nodules? *American Journal of Otolaryngology* 2008 **29** 113–118. (doi:10.1016/j.amjoto.2007.04.006)

15 Traugott AL, Dehdashti F, Trinkaus K, Cohen M, Fialkowski E, Quayle F, Hussain H, Davila R, Ylagan L & Moley JF. Exclusion of malignancy in thyroid nodules with indeterminate fine-needle aspiration cytology after negative 18F-fluorodeoxyglucose positron emission tomography: interim analysis. *World Journal of Surgery* 2010 **34** 1247–1253. (doi:10.1007/s00268-010-0398-3)

16 Kim JM, Ryu JS, Kim TY, Kim WB, Kwon GY, Gong G, Moon DH, Kim SC, Hong SJ & Shong YK. 18F-Fluorodeoxyglucose positron emission tomography does not predict malignancy in thyroid nodules cytologically diagnosed as follicular neoplasm. *Journal of Clinical Endocrinology and Metabolism* 2007 **92** 1630–1634. (doi:10.1210/jc.2006-2311)

17 Giovanella L, Suriano S, Maffioli M & Ceriani L. 18FDG-positron emission tomography/computed tomography (PET/CT) scanning in thyroid nodules with nondiagnostic cytology. *Clinical Endocrinology* 2011 **74** 644–648. (doi:10.1111/j.1365-2265.2011.04005.x).

18 Deandreis D, Al Ghuzlan A, Auperin A, Vielh P, Caillou B, Chami L, Lumbroso J,Travagli JP, Hartl D, Baudin E *et al*. Is(18)F-fluorodeoxyglucose-PET/CT useful for the presurgical characterization of thyroid nodules with indeterminate fine needle aspiration cytology? *Thyroid* 2012 **22** 165–72. (doi:10.1089/thy.2011.0255)

19 Paparo F, Corradi F, Cevasco L, Revelli M, Marziano A, Molini L, Cenderello G, Cassola G & Rollandi GA. Real-time elastography in the assessment of liver fibrosis: a review of qualitative and semi-quantitative methods for elastogram analysis. *Ultrasound in Medicine and Biology* 2014 **40** 1923–33. (doi:10.1016/j.ultrasmedbio.2014.03.021)

20 Paparo F, Cevasco L, Zefiro D, Biscaldi E, Bacigalupo L, Balocco M, Pongiglione M, Banderali S, Forni GL & Rollandi GA. Diagnostic value of real-time elastography in the assessment of hepatic fibrosis in patients with liver iron overload. *European Journal of Radiology* 2013 **82** e755–61. (doi:10.1016/j.ejrad.2013.08.038)

21 Boi F, Lai ML, Deias C, Piga M, Serra A, Uccheddu A, Faa G & Mariotti S. The usefulness of 99mTc-SestaMIBI scan in the diagnostic evaluation of thyroid nodules with oncocytic cytology. *European Journal of Endocrinology* 2003 **149** 493–498. (doi:10.1530/eje.0.1490493)

22 Vattimo A, Bertelli P, Cintorino M, Burroni L, Volterrani D, Vella A & Lazzi S. Hürthle cell tumor dwelling in hot thyroid nodules: preoperative detection with technetium-99m-MIBI. *Journal of Nuclear Medicine* 1998 **39** 822–825.

23 Bertagna F, Treglia G, Piccardo A & Giubbini R. Diagnostic and clinical significance of F-18-FDG-PET/CT thyroid incidentalomas. *Journal of Clinical Endocrinology and Metabolism* 2012 **97** 3866–3875. (doi:10.1210/jc.2012-2390).

24 Treglia G, Bertagna F, Sadeghi R, Verburg FA, Ceriani L & Giovanella L. Focal thyroid incidental uptake detected by ^{18}F-fluorodeoxyglucose positron emission tomography. Meta-analysis on prevalence and malignancy risk. *Nuklearmedizin* 2013 **52** 130–6. (doi:10.3413/Nukmed-0568-13-03)

25 Vriens D, Adang EM, Netea-Maier RT, Smit JW, de Wilt JH, Oyen WJ & de Geus-Oei LF. Cost-effectiveness of FDG-PET/CT for cytologically indeterminate thyroid nodules: a decision analytic approach. *Journal of Clinical Endocrinology and Metabolism* 2014 **99** 3263–74. (doi:10.1210/jc.2013-3483)

26 Yoo WS, Choi HS, Cho SW, Moon JH, Kim KW, Park HJ, Park SY, Choi SI, Choi SH, Lim S *et al*. The role of ultrasound findings in the management of thyroid nodules with atypia or follicular lesions of undetermined significance. *Clinical Endocrinology* 2014 **80** 735–42. (doi:10.1111/cen.12348)

27 De Nicola H, Szejnfeld J, Logullo AF, Borri Wolosker AM, Marquez F Souza LRMF & Chiferi V. Flow pattern and vascular resistive index as predictors of malignancy risk in thyroid follicular neoplasm. *Journal of Ultrasound in Medicine* 2005 **24** 897–904.

28 Treglia G, Caldarella C, Saggiorato E, Ceriani L, Orlandi F, Salvatori M & Giovanella L. Diagnostic performance of (99m)Tc-MIBI scan in predicting the malignancy of thyroid nodules: a meta-analysis. *Endocrine* 2013 **44** 70–78. (doi:10.1007/s12020-013-9932-z)

29 Giovanella L, Campenni A, Treglia G, Verburg FA, Trimboli P, Ceriani L & Bongiovanni M. Molecular imaging with ^{99m}Tc-MIBI and molecular testing for mutations in differentiating benign from malignant follicular neoplasm: a prospective comparison. *European Journal of Nuclear Medicine and Molecular Imaging* In Press. (doi:10.1007/s00259-015-3285-1)

30 Cibas ES & Ali SZ. The Bethesda system for reporting thyroid cytopathology. *Thyroid* 2009 **19** 1159–1165. (doi:10.1089/thy.2009.0274)

31 Sager S, Vatankulu B, Erdogan E, Mut S, Teksoz S, Ozturk T, Sonmezoglu K & Kanmaz B. Comparison of F-18 FDG-PET/CT and Tc-99m MIBI in the preoperative evaluation of cold thyroid nodules in the same patient group. *Endocrine* 2015 **50** 138–145. (doi:10.1007/s12020-015-0580-3)

32 Heinzel A, Müller D, Behrendt FF, Giovanella L, Mottaghy FM & Verburg FA. Thyroid nodules with indeterminate cytology: molecular imaging with 99mTc-methoxyisobutylisonitrile (MIBI) is more cost-effective than the Afirma gene expression classifier. *European Journal of Nuclear Medicine and Molecular Imaging* 2014 **41** 1497–1500. (doi:10.1007/s00259-014-2760-4)

33 Trimboli P, Treglia G & Giovanella L. Preoperative measurement of serum thyroglobulin to predict malignancy in thyroid nodules: a systematic review. *Hormones and Metabolic Research* 2015 **47** 247–52. (doi:10.1055/s-0034-1395517)

34 Xing M, Alzahrani AS, Carson KA, Viola D, Elisei R, Bendlova B, Yip L, Mian C, Vianello F, Tuttle RM *et al*. Association between BRAF V600E mutation and mortality in patients with papillary thyroid cancer. *Journal of American Medical Association* 2013 **309** 1493–1501. (doi:10.1001/jama.2013.3190)

35 Robbins RJ, Wan Q, Grewal RK, Reibke R, Gonen M, Strauss HW, Tuttle RM, Drucker M & Larson SM. Real-time prognosis for metastatic thyroid carcinoma based on 2-(18F)fluoro-2-deoxy-D-glucose-positron emission tomography scanning. *Journal of Clinical Endocrinology and Metabolism* 2006 **91** 498–505. (doi:10.1210/jc.2005-1534)

36 Piccardo A, Puntoni M, Bertagna F, Treglia G, Foppiani L, Arecco F, Giubbini R, Naseri M, Cistaro A, Cabria M *et al*. ^{18}F-FDG uptake as a prognostic variable in primary differentiated thyroid cancer incidentally detected by PET/CT: a multicentre study. *European Journal of Nuclear Medicine and Molecular Imaging* 2014 **41** 1482–91. (doi:10.1007/s00259-014-2774-y)

37 Nagarajah J, Ho AL, Tuttle RM, Weber WA & Grewal RK. Correlation of BRAFV600E mutation and glucose Metabolism in thyroid cancer patients: An^{18}F-FDG PET Study. *Journal of Nuclear Medicine* 2015 **56** 662–7 (doi:10.2967/jnumed.114.150607)

38 Trimboli P, Bongiovanni M, Rossi F, Guidobaldi L, Crescenzi A, Ceriani L, Nigri G, Valabrega S, Romanelli F & Giovanella L. Differentiated thyroid cancer patients with a previous indeterminate (Thy 3) cytology have a better prognosis than those with suspicious or malignant FNAC reports. *Endocrine* 2015 **49** 191–195 (doi:10.1007/s12020-014-0453-1)

39 Ozdemir S, Uludag A, Silan F, Atik SY, Turgut B & Ozdemir O. Possible roles of the xenobiotic transporter P-glycoproteins encoded by the MDR1 3435 C>T gene polymorphism in differentiated thyroid cancers. *Asian Pacific Journal of Cancer Prevention* 2013 **14** 3213–3217. (doi:10.7314/APJCP.2013.14.5.3213)

40 Hurtado-Lopez LM & Martinez-Duncker C. Negative MIBI thyroid scans exclude differentiated and medullary thyroid cancer in 100% of patients with hypofunctioning thyroid nodules. *European Journal of Nuclear Medicine and Molecular Imaging* 2007 **34** 1701–1703. (doi:10.1007/s00259-007-0490-6)

Received 8 December 2015
Revised version received 3 February 2016
Accepted 19 February 2016